1700°C Isothermal Phase Diagram of the MgO-Al$_2$O$_3$-TiO$_2$ System in Air Related to Pseudobrookite and Spinel Ceramics

YUCHAO QIU [1,2,4] JUNJIE SHI [1,2,5] CHANGLE HOU,[1,2,6] JINGJING DONG,[1,2,7] YUMO ZHAI,[1,2,8] KAIXUAN LI,[1,2,9] SEN YAN,[1,2,10] KAI YU,[1,2,11] JIANZHONG LI,[1,2,12] and CHANGSHENG LIU[3,13]

1.—Key Laboratory for Ecological Metallurgy of Multimetallic Mineral (Ministry of Education), Northeastern University, Shenyang 110819, People's Republic of China. 2.—School of Metallurgy, Northeastern University, Shenyang 110819, People's Republic of China. 3.—School of Material Science and Engineering, Northeastern University, Shenyang 110819, Liaoning, People's Republic of China. 4.—e-mail: qiuyc2004@126.com. 5.—e-mail: junjieshi@126.com. 6.—e-mail: 2171586@stu.neu.edu.cn. 7.—e-mail: 2171562@stu.neu.edu.cn. 8.—e-mail: yumozhai@126.com. 9.—e-mail: 20192493@stu.neu.edu. cn. 10.—e-mail: senyan96@126.com. 11.—e-mail: yuk@smm.neu.edu.cn. 12.—e-mail: lijz@mail.neu. edu.cn. 13.—e-mail: csliu@mail.neu.edu.cn

The spinel and pseudobrookite type ceramic materials have been widely used in different industries including ceramics, refractory and metallurgy. Therefore, their physicochemical properties are important for the development of related processes. In this regard, it is important to understand the formation principles of the spinel and pseudobrookite solid solutions. In the present work, the equilibrium phase relations for the MgO-Al$_2$O$_3$-TiO$_2$ system at 1700°C in air were experimentally determined by high-temperature equilibration-quenching technique followed by XRD and SEM–EDS analyses. The pseudobrookite solid solution was found to be coexisting with spinel solid solution and rutile phase, respectively. The composition evolution and formation principles of the pseudobrookite and spinel solid solutions were further elucidated from the corresponding crystal structures and composition relations. Furthermore, great discrepancies were observed when the 1700°C isotherm from the present work was compared with the isotherm simulated by FactSage 8.1. The evolution of the solid solution existing area was intuitively presented with reference to the experimental data from the literature. The results from present work are important for the development of spinel and pseudobrookite solid solution ceramics as well as the optimization of the thermodynamic database for oxide systems.

INTRODUCTION

Due to the rapid development of fifth generation (5G) communication networks and wireless systems, the demand for polycrystalline ceramics, microwave dielectric ceramics and high-temperature ceramic materials has grown significantly.[1–3] The compounds of MgAl$_2$O$_4$ and Mg$_2$TiO$_4$ with cubic spinel structure are widely used in ceramics and microwave dielectric materials fields because of

their high erosion resistance, great abrasion resistance, excellent thermal shock stability and dielectric properties.[4–6] However, their further application in millimeter-wave communications is limited because of the low Qf (quality factor) values of MgAl$_2$O$_4$ ceramics and poor sintering capacity of Mg$_2$TiO$_4$ ceramics.[7,8] Recently, Yang et al.[9] found that the sintering ability of Mg$_2$TiO$_4$ ceramics and the microwave dielectric properties of MgAl$_2$O$_4$ ceramics were significantly improved simultaneously with the formation of the solid solution by Mg$_2$TiO$_4$ and MgAl$_2$O$_4$ at temperature higher than 1450°C. However, the formation principle of the

1700°C Isothermal Phase Diagram of the MgO-Al$_2$O$_3$-TiO$_2$ System in Air Related to
Pseudobrookite and Spinel Ceramics

1983

Mg$_2$TiO$_4$-MgAl$_2$O$_4$ solid solution was not clearly explained. In addition, the Al$_2$TiO$_5$ and MgTi$_2$O$_5$ ceramics with pseudobrookite structure characterized by high anisotropy of thermal expansion coefficients, high melting point and high thermal shock resistance are widely used in heat exchanger and thermistor and polycrystalline ceramics fields.[10–13] Recently, Kornaus[14] reported that the Al$_2$TiO$_5$-MgTi$_2$O$_5$ solid solution was formed by the introduction of MgTi$_2$O$_5$ into Al$_2$TiO$_5$. The thermal shock resistance and thermal stability of Al$_2$TiO$_5$ were effectively improved accordingly. However, the formation principle of Al$_2$TiO$_5$-MgTi$_2$O$_5$ (pseudobrookite) solid solution also remains unclear. Furthermore, MgAl$_2$O$_4$, Mg$_2$TiO$_4$, Al$_2$TiO$_5$ and MgTi$_2$O$_5$ all show fairly high melting points of 2135°C, 1732°C, 1652°C and 1860°C, respectively, leading to the formation of the corresponding solid solution becoming more difficult if the sinter temperature is not high enough.[15,16] It is necessary to systematically explore the formation principles of spinel and pseudobrookite solid solutions at high temperature, which will provide the basis for a wide application of the ceramics formed by spinel and pseudobrookite solid solutions.

It is well known that the evolution of the equilibrium phase relations with composition and temperature can be visually observed from the phase diagram. Therefore, the understanding of the thermodynamic properties of Mg$_2$TiO$_4$-MgAl$_2$O$_4$ and Al$_2$TiO$_5$-MgTi$_2$O$_5$ solid solutions will become easier if the phase diagram of MgO-Al$_2$O$_3$-TiO$_2$ system has been well established. During the past decades, the core binary systems of MgO-Al$_2$O$_3$,[17,18] MgO-TiO$_2$[19,20] and Al$_2$O$_3$-TiO$_2$[21,22] have been extensively investigated by using the high-temperature equilibration-quenching experiment, DTA (differential thermal analysis) and DSC (differential scanning calorimetry). However, investigations of the equilibrium phase relations for MgO-Al$_2$O$_3$-TiO$_2$ system are relatively limited, especially for the temperature range > 1550°C. Boden et al.[23] investigated MgO-Al$_2$O$_3$-TiO$_2$ system by using x-ray powder diffraction and a focusing camera with a powder diffractometer at 1300°C and 1550°C, and the results indicated that the continuous solid solutions were formed between MgTiO$_5$ and Al$_2$TiO$_5$, MgAl$_2$O$_4$ and Mg$_2$TiO$_4$, respectively. Hauck[24] carried out MgO-Al$_2$O$_3$-TiO$_2$ system by structure model at 1000°C to 1400°C. Limited solid solutions of MgTiO$_3$ and Al$_2$O$_3$ were indicated at 1400°C, and the three phase triangles turned in a counterclockwise direction with decreasing temperature. Ilatovskaia et al.[19] determined the phase relations of the ternary system by x-ray diffraction, scanning electron microscopy with an energy dispersive x-ray analysis, DTA and DSC at 996°C to 1424°C, and the experimental results were similar to the data by Boden et al.[23] In summary, spinel and pseudobrookite solid solutions were found by different experimental methods at 1000°C to 1550°C.

However, the dimensions of solid solution region varied with temperature, and the formation principles of solid solutions were not clearly clarified. Nowadays, the CALPHAD technique has been frequently used to predict the thermodynamic properties of the ceramics. In 1988, Kaufman[25] tried to calculate the phase diagram for MgO-Al$_2$O$_3$-TiO$_2$ system; however, the effects of extensive solid solution formation particularly in MgAl$_2$O$_4$ spinel were not considered, leading to a considerable liquid area compared with the experimental results. With the rapid progress of the thermodynamic models and computer techniques, the commercial thermodynamic software packages including FactSage, MTDATA, etc., have been developed. However, the accuracy of the database is mainly based on the reliability of experimental data from low-order systems, and the accuracy predictions of the equilibrium phase relations for high-order systems remain unclear. Moreover, most of the previous studies were focused on the equilibrium phase relation at temperature < 1550°C, while the information at higher temperatures is relatively less, which would be of use for more direct explanation of the formation principles of the Mg$_2$TiO$_4$-MgAl$_2$O$_4$ and Al$_2$TiO$_5$-MgTi$_2$O$_5$ solid solutions used in the ceramics industry.

Consequently, the present work focused on investigating the phase equilibria of the MgO-Al$_2$O$_3$-TiO$_2$ system at 1700°C in air. High-temperature equilibration-quenching technique with the analysis of x-ray powder diffraction (XRD) and scanning electron microscopy with an energy dispersive x-ray (SEM–EDS) were applied. Special attention was paid to the discussion of formation principles of the Mg$_2$TiO$_4$-MgAl$_2$O$_4$ and Al$_2$TiO$_5$-MgTi$_2$O$_5$ solid solutions. The results from the present work are not only useful in the ceramics industry, but also important to update current oxide thermodynamic databases.

EXPERIMENTAL

Each sample weighing about 0.4 g was a mixture of high-purity powders of MgO (Sinopharm Reagent 99.9 wt.% pure), Al$_2$O$_3$ (Sinopharm Reagent 99.99 wt.% pure) and TiO$_2$ (Aladdin 99.0 wt.% pure), with the pre-calculated proportions. The mixture was then ground homogeneously in an agate mortar for at least 15 min and pressed into a cylindrical pellet using a stainless-steel tool at a pressure of 3 MPa. Afterwards, the pellet was placed in a Pt sheet with length of 8 mm, width of 8 mm and thickness of 0.15 mm. More experimental details can be found from our previous publications.[26–30]

The high-temperature equilibration process for the sample was conducted in an electrical MoSi$_2$ resistance heated furnace. A calibrated B-type thermocouple with an overall accuracy estimated to within ± 3°C was placed next to the sample to

monitor the temperature within the homogeneous zone. The sample was first heated to 1710°C for 30 min to promote the diffusion and homogenization of the oxide powder, after which the temperature was decreased to 1700°C and kept for a sufficient period until the sample reach the equilibrium state. It has been confirmed that 24 h was sufficient for the reach of equilibration from the preliminary experiments according to the varying of the compositions and microphotograph of the coexisting phases.[31] After reaching equilibration, the sample was quenched in an ice-water mixture to avoid a decline of temperature, and the phase assembly state at high temperature could be retained at room temperature. The quenched sample was dried and stored in a drying vessel for further analysis.

It is well known that the valence states of titanium can vary with temperature and oxygen partial pressure as Ti^{2+}, Ti^{3+} and Ti^{4+}, respectively. It is therefore essential to verify the valence state of Ti in the present work. According to the Ti-O predominance area diagram in Fig. 1 calculated by FactSage 8.1 with the "Phase Diagram" module and "FactPS" databases,[32] titanium can be stable as Ti, TiO, Ti_2O_3, Ti_3O_5 and Magnéli phase (Ti_nO_{2n-1}, $4 \leq n \leq 10$) or TiO_2 with the varying temperature and oxygen partial pressure. Under the experimental parameters of 1700°C and air atmosphere in the present study, the valence state of titanium was confirmed as Ti^{4+}, as shown by the projection of point A in Fig. 1; therefore, the oxide form of Ti and TiO_2 can be presented during the following discussion.

The quenched sample was randomly divided into two parts; one part was mounted in resin, ground, polished by wet metallographic and gold-coated using an ion coater (Hitachi E1045, Japan) to increase its electrical conductivity. The other part was ground to a powder in preparation for x-ray diffraction (XRD). Scanning electron microscope (SEM, Quanta250FEG) coupled with an energy-dispersive x-ray spectrometer (EDS, Oxford SSD)
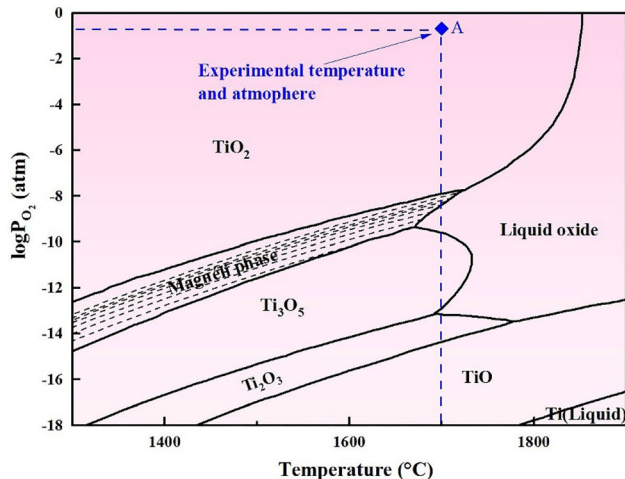
was used for characterizing the equilibrium micrographs and compositions with an accelerating voltage of 20 kV, a beam current of 10 nA and a working distance of 10 mm. The external standards utilized in the EDS analyses were metallic magnesium (for Mg, Kα), metallic aluminum (for Al, Kα), rutile (for Ti, Kα) and olivine (for O, Kα). At least six points or areas were randomly selected for each individual phase to achieve high accuracy. A D8-Advance using Cu Ka radiation at a scan rate of 2°/min from 10° to 80° (acceleration voltage 40 kV and current 30 mA) was selected to further determined composition of each sample; the crystal structures of the phases were identified by Search-Match software, version 2.1.1.0, based on the PDF2004 card database.[33]

RESULTS AND DISCUSSION

Equilibrium Phase Relations

The SEM micrographs, compositions as well as corresponding typical XRD diffraction patterns of the equilibrium phase for the $MgO-Al_2O_3-TiO_2$ system at 1700°C in air are presented in Fig. 2, Table I and Fig. 3, respectively. In the composition range studied in the present work, two different extensive solid solutions were found, which were identified as pseudobrookite solid solution and spinel solid solution. The corresponding general formulas can be described as $(MgTi_2O_5, Al_2TiO_5)_{ss}$ and $(Mg_2TiO_4, MgAl_2O_4)_{ss}$, respectively, based on the consistence of the equilibrium composition in Table I and the XRD patterns in Fig. 3. Furthermore, two different two-phase coexisting equilibria were identified as pseudobrookite-rutile and pseudobrookite-spinel. In Fig. 2a, b, c, d, e, and f, the pseudobrookite-spinel solid solution equilibrium assembly is presented, and the spinel phase was observed as an irregular polygon. In Fig. 2g, an example of a pseudobrookite–rutile coexisting equilibrium is shown by sample AMT7; the matrix was confirmed as pseudobrookite, while the rutile was shown as elongated.

Formation Principles of Spinel and Pseudobrookite Solid Solutions

The spinel and pseudobrookite ceramics are widely used in various engineering fields because of the excellent combination properties generated by the formation of solid solutions. Table I shows that the compositions of spinel and pseudobrookite solid solutions found in the present work varied greatly even though the same crystal structures were confirmed by the XRD diffraction peaks in Fig. 3b. Moreover, the diffraction peaks between 17°–20° and 25°–27° also exhibited a slightly rightward-shifting trend for the solid solutions. Similar results were reported by Yang et al.[9] that the XRD peak position and intensity varied with temperature and composition for spinel solid solution. Both the
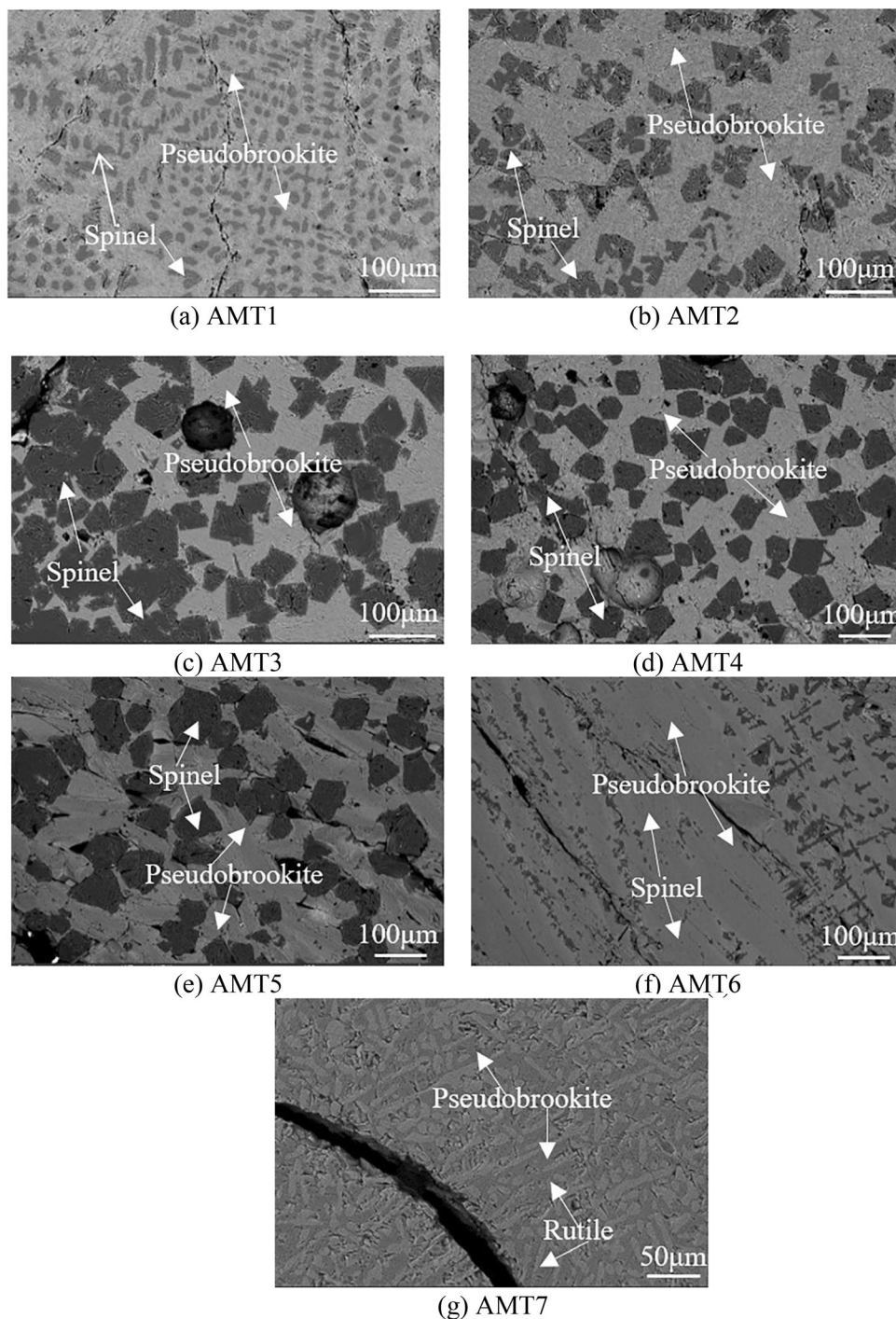

Fig. 1. Ti-O predominance area diagram.

1700°C Isothermal Phase Diagram of the MgO-Al$_2$O$_3$-TiO$_2$ System in Air Related to Pseudobrookite and Spinel Ceramics

1985

Fig. 2. Microstructures of the equilibrium phases in air at 1700°C in the MgO-Al$_2$O$_3$-TiO$_2$ system.

results from present study and the literature indicated that there should be a relationship between the composition with the corresponding structure. It is important for the understanding of the formation principles of spinel and pseudobrookite solid solution phases.

The physical properties and crystal structures of the end elements in solid solutions are key to clarify the formation principles of solid solution. The space group of MgAl$_2$O$_4$ and Mg$_2$TiO$_4$ both belong to $Fd3m$, and the densities are 3.550 g cm^{-3} and 3.520 g cm^{-3}, respectively.[34] Furthermore, MgAl$_2$O$_4$ belongs to the normal spinel with the structural formula of Mg^{2+}[Al$_2^{3+}$]O$_4$, as shown Fig. 4a, where Mg^{2+} and Al^{3+} occupy the tetrahedral (T) and octahedral (O) sites in the crystal lattice, respectively,[35] while Mg$_2$TiO$_4$ belongs to the inverse spinel with the structural formula of Mg^{2+}[Mg^{2+}Ti^{4+}]O$_4$,
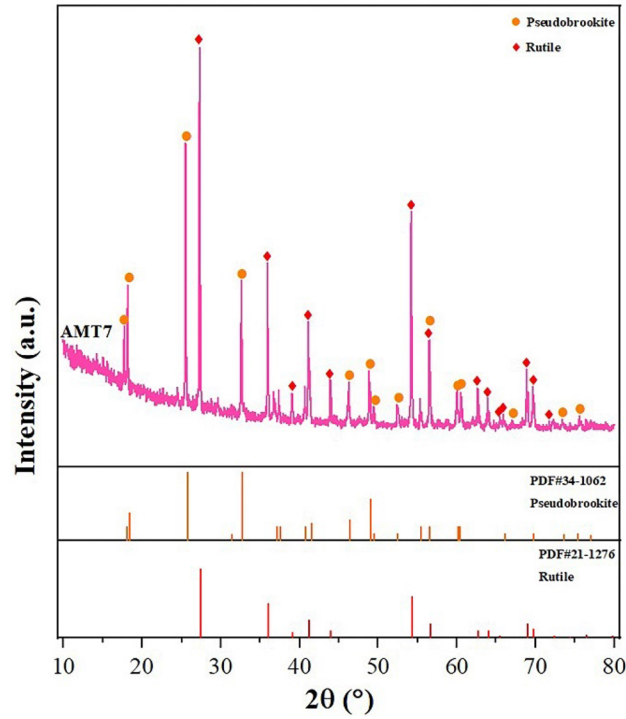
Table I. Compositions of the equilibrium phases at 1700°C in air for MgO-Al$_2$O$_3$-TiO$_2$ system

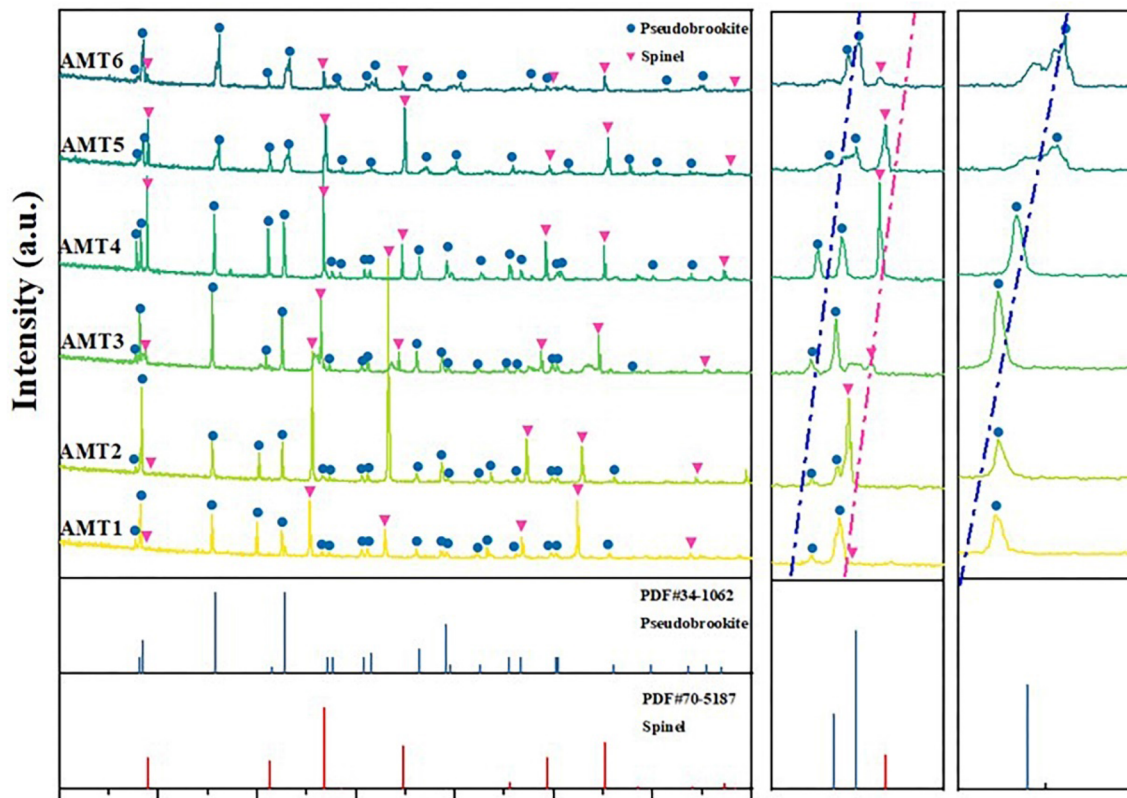| No	Initial compositions, wt.%			Equilibrium phases	Stoichiometric formula	Equilibrium compositions, wt.%		
	MgO	Al$_2$O$_3$	TiO$_2$			MgO	Al$_2$O$_3$	TiO$_2$
AMT1	38.0	5.0	57.0	Pseudobrookite	$([Al_2^{3+}Ti^{4+}][Al_2^{3+}Ti_2^{4+}]O_5)_{0.05}(Mg^{2+}[Ti_2^{4+}]O_5)_{0.95}$	27.4 ± 0.3	3.4 ± 0	69.2 ± 0.3
				Spinel	$(Mg^{2+}[Mg^{2+}Ti^{4+}]O_4)_{0.9}(Mg^{2+}[Al_2^{3+}]O_4)_{0.1}$	44.4 ± 0.1	7.1 ± 0.1	48.4 ± 0.1
AMT2	37.0	13.0	50.0	Pseudobrookite	$([Al_2^{3+}Ti^{4+}][Al_2^{3+}Ti_2^{4+}]O_5)_{0.1}(Mg^{2+}[Ti_2^{4+}]O_5)_{0.9}$	24.4 ± 0.1	6.5 ± 0.1	69.0 ± 0.3
				Spinel	$(Mg^{2+}[Mg^{2+}Ti^{4+}]O_4)_{0.75}(Mg^{2+}[Al_2^{3+}]O_4)_{0.25}$	42.1 ± 0.3	17.3 ± 0.1	40.6 ± 0.2
AMT3	28.0	25.0	47.0	Pseudobrookite	$([Al_2^{3+}Ti^{4+}][Al_2^{3+}Ti_2^{4+}]O_5)_{0.12}(Mg^{2+}[Ti_2^{4+}]O_5)_{0.88}$	21.1 ± 0.3	7.6 ± 0.4	71.3 ± 0.7
				Spinel	$(Mg^{2+}[Mg^{2+}Ti^{4+}]O_4)_{0.2}(Mg^{2+}[Al_2^{3+}]O_4)_{0.8}$	31.5 ± 0.2	57.5 ± 0.5	11.0 ± 0.6
AMT4	20.0	37.0	43.0	Pseudobrookite	$([Al_2^{3+}Ti^{4+}][Al_2^{3+}Ti_2^{4+}]O_5)_{0.31}(Mg^{2+}[Ti_2^{4+}]O_5)_{0.69}$	13.7 ± 0.2	15.6 ± 0.2	70.2 ± 0.6
				Spinel	$(Mg^{2+}[Mg^{2+}Ti^{4+}]O_4)_{0.034}(Mg^{2+}[Al_2^{3+}]O_4)_{0.966}$	27.0 ± 0.1	71.1 ± 0.0	1.9 ± 0.0
AMT5	13.0	50.0	37.0	Pseudobrookite	$([Al_2^{3+}Ti^{4+}][Al_2^{3+}Ti_2^{4+}]O_5)_{0.74}(Mg^{2+}[Ti_2^{4+}]O_5)_{0.26}$	5.2 ± 0.1	41.4 ± 0.5	53.3 ± 0.7
				Spinel	$(Mg^{2+}[Mg^{2+}Ti^{4+}]O_4)_{0.038}(Mg^{2+}[Al_2^{3+}]O_4)_{0.962}$	18.7 ± 0.3	78.7 ± 0.2	2.6 ± 0.5
AMT6	10.0	38.0	52.0	Pseudobrookite	$([Al_2^{3+}Ti^{4+}][Al_2^{3+}Ti_2^{4+}]O_5)_{0.76}(Mg^{2+}[Ti_2^{4+}]O_5)_{0.24}$	5.4 ± 0.6	40.5 ± 0.5	54.0 ± 0.8
				Spinel	$(Mg^{2+}[Mg^{2+}Ti^{4+}]O_4)_{0.041}(Mg^{2+}[Al_2^{3+}]O_4)_{0.959}$	26.1 ± 0.1	71.7 ± 0.2	2.2 ± 0.1
AMT7	7.7	4.3	88.0	Pseudobrookite	$([Al_2^{3+}Ti^{4+}][Al_2^{3+}Ti_2^{4+}]O_5)_{0.19}(Mg^{2+}[Ti_2^{4+}]O_5)_{0.81}$	19.1 ± 0.2	2.3 ± 0.3	78.6 ± 0.4
				Rutile	TiO$_2$	27.4 ± 0.3	3.4 ± 0	69.2 ± 0.3

where the T-sites are completed occupied by the Mg^{2+} and O-sites, which are equally occupied by Mg^{2+} and Ti^{4+} in Fig. 4b. As the temperature increased, the inversion of the spinel structure occurred[36] by the transformation of normal spinel to inverse spinel, and vice versa. In general, the compounds with the same space group, similar density and ionic radius trend to forming solid solution phase.[37,38] Therefore, the formation reaction of the spinel solid solution in the present study can be represented by following reaction of xMg^{2+}[Al$_2^{3+}$]O$_4$ + $(1-x)$Mg^{2+}[Mg^{2+}Ti^{4+}]O$_4$ → Mg^{2+}[Al$_{2x}^{3+}$ Mg$_{1-x}^{2+}$Ti$_{1-x}^{4+}$]O$_4$($0 \leq x \leq$ 1). Furthermore, the formula of the formed spinel solid solution was calculated according to the mole ratios of Mg: Al: Ti, as listed in Table I. Meanwhile, the composition relations of Ti and Al varying with Mg are presented in Fig. 5a; the varying tendencies consisted of a liner relation, and with the increase of Mg content from 34.6 wt.% to 63.33 wt.%, the Al content decreased greatly from 64.13 wt.% to 6.67 wt.% and the Ti content increased from 1.27 wt.% to 30 wt.% in the spinel solid solution. Within the current composition range, the equations for the variation of Al and Ti content with Mg content were derived as $w_{Ti} = w_{Mg}$-33.33 and w_{Al} = -2w_{Mg} + 133.33, respectively.

Microscopic and macroscopic cracks are easily formed during the sintering process for Al$_2$TiO$_5$ ceramics, mainly because of the thermal stresses on grain boundaries generated by anisotropic contraction, while the cracks can be efficiently improved by the addition of Mg element to facilitate the formation of pseudobrookite solid solution.[43,44] As one of the end members, Al$_2$TiO$_5$ belongs to *Ccmm* space group as inverse pseudobrookite with density of 3.770 g cm^{-3}.[45] As shown Fig. 4c, Al$_2$TiO$_5$ can be expressed as the general formula of [Al$_2^{3+}$ Ti^{4+}][Al$_2^{3+}$ Ti^{4+}]O$_5$ as Al^{3+} and Ti^{4+} together occupy the cationic site. For another end member, MgTi$_2$O$_5$ belongs to *Bbmm* space group as normal pseudobrookite with density of 3.647 g cm^{-3}.[46] In Fig. 4d for the crystal lattice of MgTi$_2$O$_5$, the M1 octahedra sites are completely occupied by Mg^{2+}, while M2 octahedra sites are occupied by Ti^{4+}, and MgTi$_2$O$_5$ is therefore expressed as Mg^{2+}[Ti$_2^{4+}$]O$_5$. The similar inversion effect that happened to spinel solid solution is also found for pseudobrookite during the temperature increase, resulting in the O-sites and T-sites being jointly occupied by Al^{3+}, Mg^{2+} and Ti^{4+}, respectively.[47] The formation reaction of the pseudobrookite solid solution can be represented by following reaction of x[Al$_2^{3+}$ Ti^{4+}][Al$_2^{3+}$ Ti^{4+}]O$_5$ + $(1-x)$Mg^{2+}[Ti$_2^{4+}$]O$_5$ → (Al$_{2x}^{3+}$Mg$_{1-x}^{2+}$Ti$_{2-x}^{4+}$)$_1^O$(Al$_{2x}^{3+}$Mg$_{1-x}^{2+}$Ti$_{2-x}^{4+}$)$_2^T$(O^{2-})$_5$ ($0 \leq x \leq 1$). Furthermore, a similar concentration relationship discussed for spinel solid solution was found for pseudobrookite solid solution, as shown in Fig. 5b. According to the atomic ratio of Mg, Al and Ti, the variations of Al and Ti content

1700°C Isothermal Phase Diagram of the MgO-Al$_2$O$_3$-TiO$_2$ System in Air Related to
Pseudobrookite and Spinel Ceramics

1987

system.

(a) XRD diffraction patterns for the sample AMT7

(b) XRD diffraction patterns for samples AMT1-AMT6

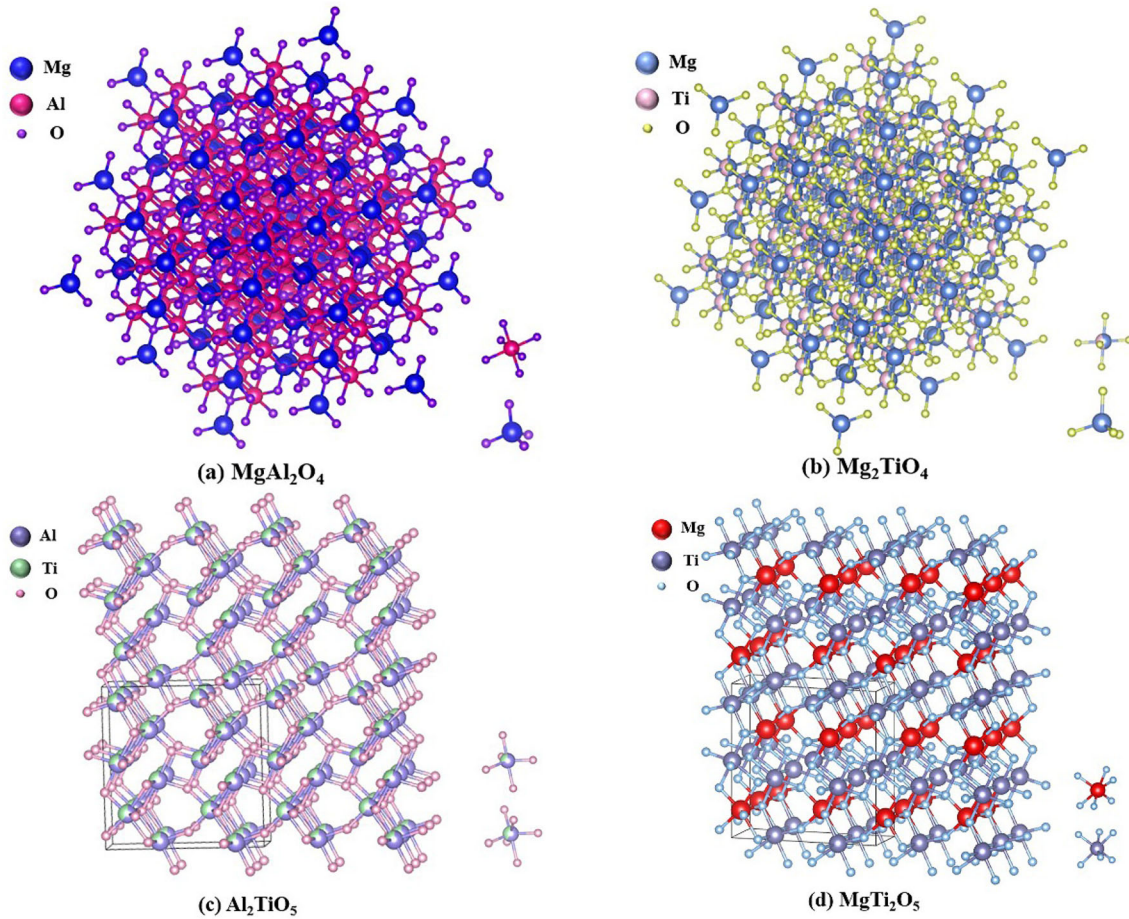Fig. 3. XRD diffraction patterns for the equilibrium phases of MgO-Al$_2$O$_3$-TiO$_2$ system at 1700°C in air.

Fig. 4. Crystal structure diagram of $MgAl_2O_4$,[39] Mg_2TiO_4,[40] Al_2TiO_5[41] and $MgTi_2O_5$.[42]
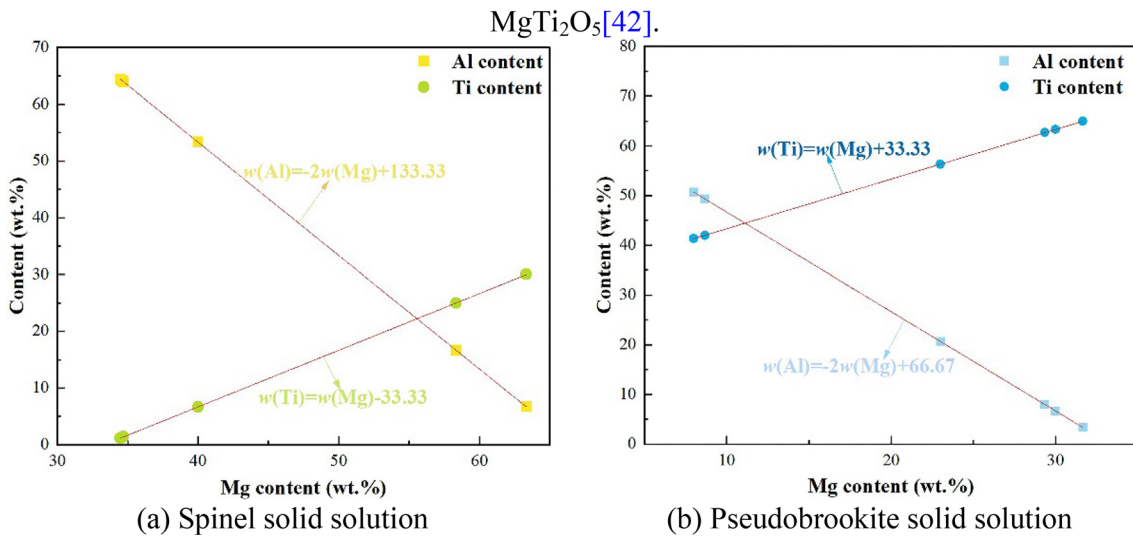
Fig. 5. The variation of Al content and Ti content with Mg content for pseudobrookite and spinel solid solutions.

with Mg content were expressed as $w_{Ti} = w_{Mg} + 33.33$ and $w_{Al} = -2w_{Mg} + 66.67$, respectively. With the Mg content increased from 8.0 wt.% to 31.68 wt.% in the pseudobrookite solid solution,

the Al content decreased from 50.67 wt.% to 3.33 wt.%, while the Ti content increased from 41.33 wt.% to 65.0 wt.%.

Projections of the 1700°C Isotherm

According to the equilibrium phase relations and compositions mentioned above, the 1700°C isothermal phase diagram was constructed for the ternary MgO-Al$_2$O$_3$-TiO$_2$ system and presented in Fig. 6. Two kinds of two-phase coexistence regions were experimentally identified, as indicated by the tie lines for the rutile-pseudobrookite and spinel-pseudobrookite coexisting areas. The light green area in Fig. 6 was labeled as spinel-periclase coexisting according to the thermodynamic principle. In the phase diagram, rutile, pseudobrookite, spinel and periclase were abbreviated as Rt., Pse., Spl. and Per., respectively, in accordance with "Abbreviations for Names of Rock-forming Minerals."[48]

Comparisons of the 1700°C Isotherms

The 1700°C isotherm for MgO-Al$_2$O$_3$-TiO$_2$ system was simulated by FactSage 8.1 with reference to "FactPS" and "FToxid" databases under the same experimental parameters.[32] As projected in Fig. 7a, significant discrepancies were found during the comparison between the experimental results and calculation. A considerable liquid phase region and multiple two and three phase regions associated with the liquid phase were indicated by FactSage 8.1. In contrast, only two regions of two-phase coexistence, i.e., rutile-pseudobrookite and spinel-pseudobrookite, have been experimentally confirmed. Apparently, spinel and pseudobrookite phases were not considered as solid solutions during

the optimization of the current version of the database, resulting in a reduced reference value of the database related to MgO-Al$_2$O$_3$-TiO$_2$ system. As a result, the current experimental results are useful for the improvement of the related thermodynamic oxide database.

In Fig. 7b, the 1550°C isothermal of MgO-Al$_2$O$_3$-TiO$_2$ system plotted by Boden et al.[23] was replotted for comparison with the current experimental data. There is a relatively good consistency for the distribution of spinel and pseudobrookite solid solutions, and the solid solution coexistence region showed a gradual expansion with temperature increase. However, the three-phase region of MgTiO$_3$-spinel-pseudobrookite was not found in the present work, which was caused by the decomposition of MgTiO$_3$ to MgO and TiO$_2$ as the decomposition temperature of MgTiO$_3$ was reported to be around 1640°C in previous literature.[49] Another difference is that the reported Al$_2$O$_3$-spinel-pseudobrookite three-phase coexistence region was also not determined in present study, which may be caused by the shrinkage of the area with the increase of temperature from 1550°C to 1700°C.

To have a more intuitive effect of the temperature on the distributions of two- and three-phase coexisting areas, the 1400°C and 1550°C isotherms reported by Hauck[24] and Boden et al.[23] were projected simultaneously with the 1700°C isotherm from present work, as shown in Fig. 8a and b, respectively. Hauck[24] reported that a limited solid solution formed by MgTiO$_3$ and Al$_2$O$_3$ was found at
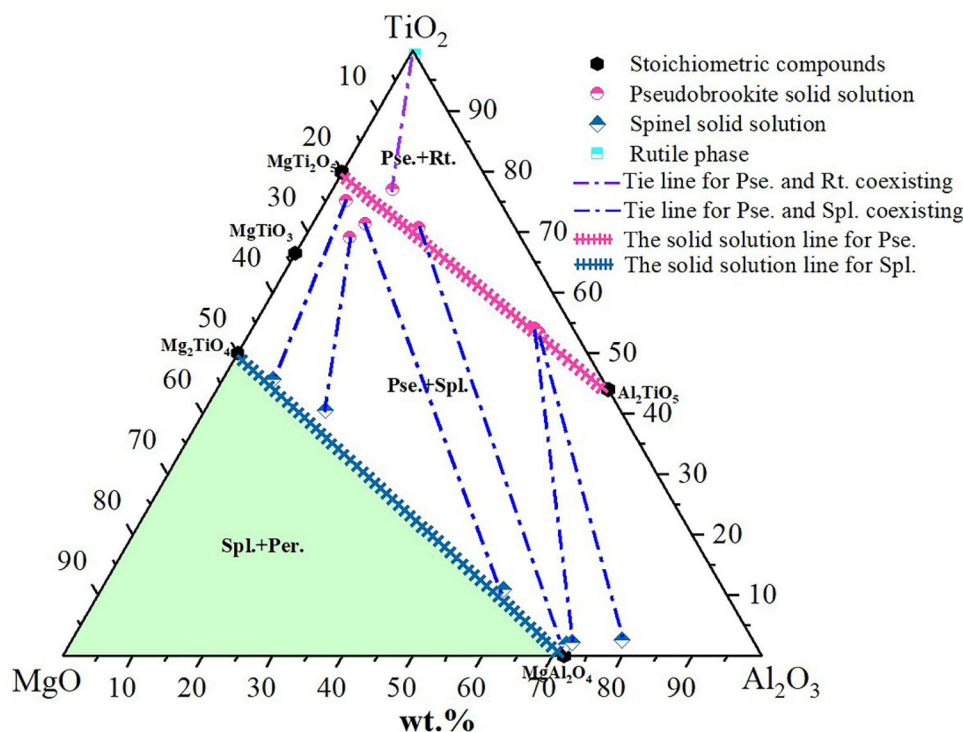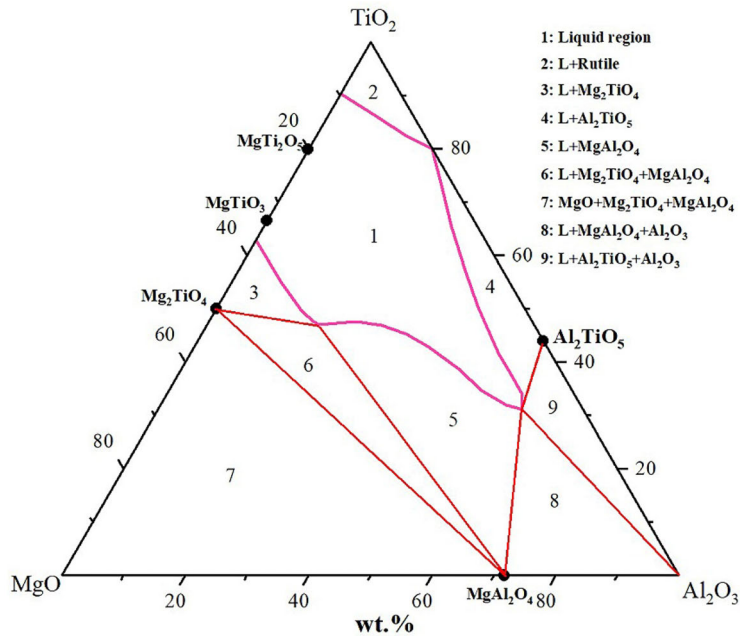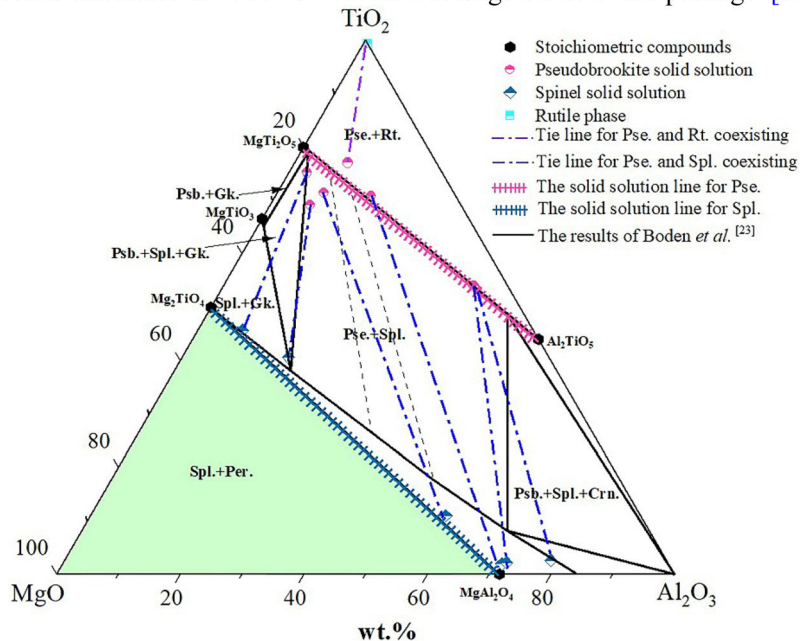

Fig. 6. Projection of the experimental equilibrium phase relations on the MgO-Al$_2$O$_3$-TiO$_2$ phase diagram at 1700°C.

(a) Results calculated at 1700 °C with the FactSage 8.1 software package. [32]

(b) Comparison of the 1550 °C isothermal phase diagram by Boden *et al*. [23] with the results from present work

Fig. 7. Comparison of the present experimental results at 1700°C with calculation[32] and literature[23] (Psb. = pseudobrookite, Rt. = rutile, Spl. = spinel, Crn. = corundum, Gk. = MgTiO$_3$, Per. = Periclase).

1400°C, which disappeared at 1550°C and 1700°C. As shown Fig. 8a, the three-phase regions of MgTiO$_3$-spinel-pseudobrookite and Al$_2$O$_3$-spinel-pseudo-brookite become progressively smaller and rotate counterclockwise with the increase of temperature. On the other hand, the spinel-pseudobrookite coexisting region became remarkably larger as the temperature increased from 1400°C to 1700°C (Fig. 8b). Therefore, to obtain a wide range of solid solutions and avoid the influence of MgTiO$_3$ and Al$_2$O$_3$ on the preparation of ceramic materials, the temperature should be increased appropriately.

1700°C Isothermal Phase Diagram of the MgO-Al$_2$O$_3$-TiO$_2$ System in Air Related to
Pseudobrookite and Spinel Ceramics

1991

(a) Variation of the three-phase coexistence regions

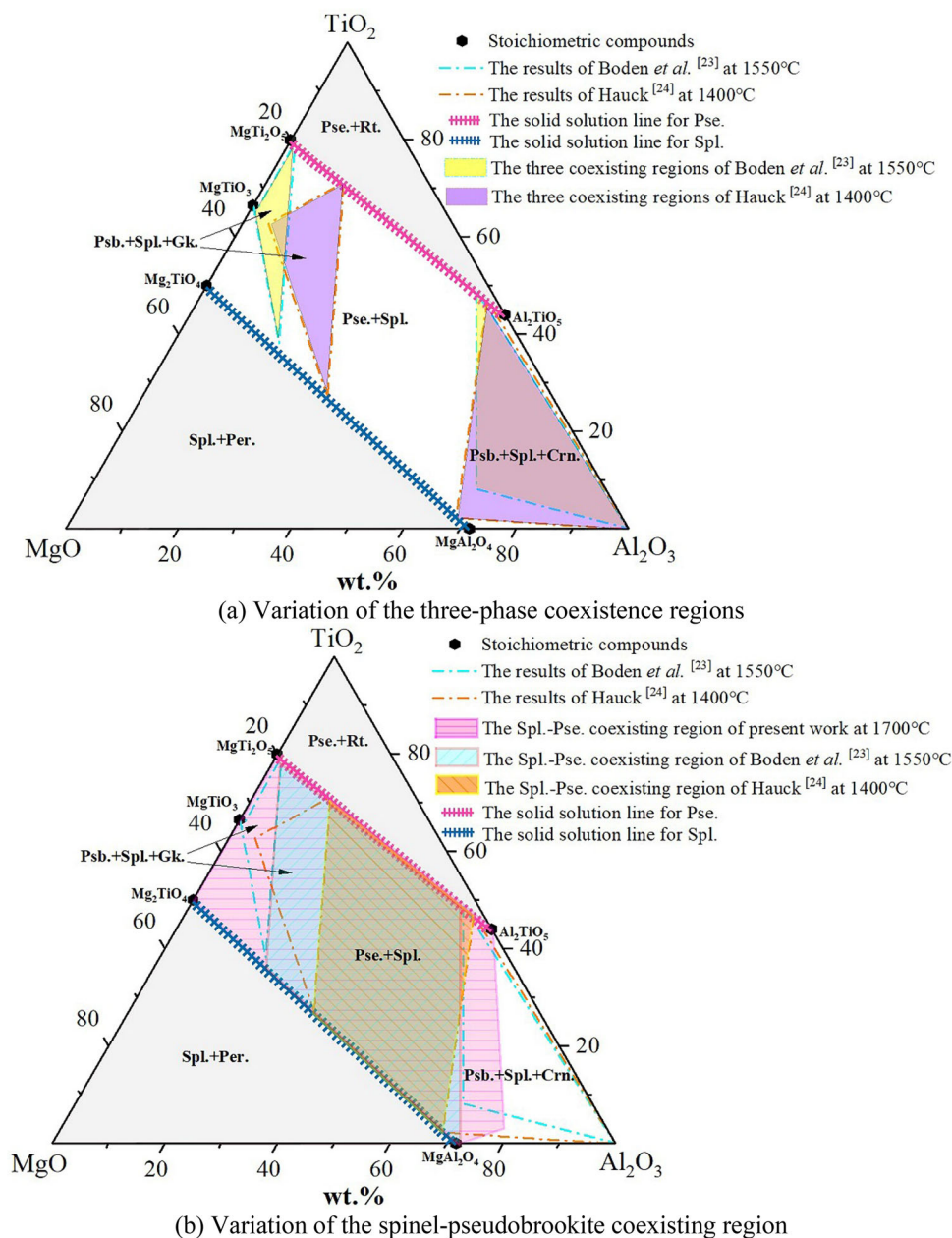(b) Variation of the spinel-pseudobrookite coexisting region

Fig. 8. Variation of the three-phase coexisting regions and spinel-pseudobrookite coexisting region with temperature.

CONCLUSION

High-temperature equilibration-quenching experiments were conducted to construct the phase diagram of MgO-Al$_2$O$_3$-TiO$_2$ system at 1700°C in air. The equilibrium phase relationships were clarified by SEM–EDS combined with XRD analysis. The pseudobrookite solid solution was confirmed to coexist with spinel solid solution and rutile phase, respectively. The composition evolution and the formation principles of spinel and pseudobrookite solid solutions were indicated by the crystal structures and physical properties of each end element. Furthermore, the variation of the three-phase coexisting regions and spinel-pseudobrookite coexisting region with temperature were clarified by comparing the present results with the previous data from literature. The current work is a useful reference for the application of spinel and pseudobrookite solid solutions in ceramics as well as providing the essential and novel phase diagram data for updating the related oxide databases of thermodynamic software tools.

CONFLICT OF INTEREST

The authors declare that they have no known competing financial interests or personal relationships that could have appeared to influence the work reported in this paper.

REFERENCES

1. B. Liu, K. Sha, Y.Q. Jia, Y.H. Huang, C.C. Hu, L. Li, D.W. Wang, D. Zhou, and K.X. Song, *J. Eur. Ceram. Soc.* 41, 4835 (2021).
2. D.H. Jin, B. Liu, K.X. Song, K.W. Xu, Y.H. Huang, C.C. Hu, and Y.Y. Hu, *J. Alloys Compd.* 886, 161141 (2021).
3. B. Liu, L. Li, K.X. Song, M.M. Mao, Z. Lu, G. Wang, L. Li, D. Wang, D. Zhou, A. Feteira, and I.M. Reaney, *J. Eur. Ceram. Soc.* 41, 1726 (2021).
4. S. Takahashi, A. Kan, and H. Ogawa, *J. Eur. Ceram. Soc.* 37, 1001 (2017).
5. O. Padmaraj, M. Venkateswarlu, and N. Satyanarayana, *Ceram. Int.* 41, 3178 (2015).
6. H. Yu, T. Luo, L. He, and J. Liu, *Adv. Appl. Ceram.* 118, 98 (2019).
7. A. Belous, O. Ovchar, D. Durilin, M.M. Krzmanc, M. Valant, and D. Suvorov, *J. Am. Ceram. Soc.* 89, 3441 (2006).
8. T. Qin, C. Zhong, Y. Qin, B. Tang, and S. Zhang, *Ceram. Int.* 46, 19046 (2020).
9. X. Yang, Y. Lai, Y. Zeng, F. Yang, F. Huang, B. Li, F. Wang, C. Wu, and H. Su, *J. Alloys Compd.* 898, 162905 (2022).
10. Y. Suzuki, and Y. Shinoda, *Sci. Technol. Adv. Mater.* 12, 034301 (2011).
11. T. Shimaz, M. Miura, N. Isu, T. Ogawa, K. Ota, H. Maeda, and E.H. Ishida, *Metall. Mater. Trans. A* 487, 340 (2008).
12. R. Papitha, M.B. Suresh, D. Das, and R. Johnson, *Process Appl. Ceram.* 7, 143 (2013).
13. S. Bueno, R. Moreno, and C. Baudin, *J. Eur. Ceram. Soc.* 24, 2785 (2004).
14. K. Kornaus, P. Rutkowski, R. Lach, and A. Gubernat, *J. Eur. Ceram. Soc.* 41, 1498 (2021).
15. L. Giordano, M. Viviani, C. Bottino, M.T. Buscaglia, V. Buscaglia, and P. Nanni, *J. Eur. Ceram. Soc.* 22, 1811 (2002).
16. G.L.M. Kristen, H. Brosnan, and D.K. Agrawal, *J. Am. Ceram. Soc.* 86, 1307 (2004).
17. I.H. Jung, S.A. Decterov, and A.D. Pelton, *J. Phase Equilib. Diff.* 25, 329 (2004).
18. A.F. Henriksen, and W.D. Kingery, *Ceramurgia Int.* 5, 11 (1979).
19. M. Ilatovskaia, I. Saenko, G. Savinykh, and O. Fabrichnaya, *J. Am. Ceram. Soc.* 101, 5198 (2018).
20. I. Shindo, *J. Cryst. Growth* 50, 839 (1980).
21. Y.J. Park, W.Y. Kim, and Y.B. Kang, *J. Eur. Ceram. Soc.* 41, 7362 (2021).
22. A. Spencer, *Oxid. Met* 35, 53 (1991).
23. G.P. Boden, and F.P. Glasser, *Trans. J. Br. Ceram. Soc* 72, 215 (1973).
24. J. Hauck, *J. Solid State Chem.* 36, 52 (1981).
25. L. Kaufman, *Physica B+C (Amsterdam)* 150, 99 (1988).
26. X. Wan, J. Shi, Y. Qiu, M. Chen, J. Li, C. Liu, P. Taskinen, and A. Jokilaakso, *Ceram. Int.* 47, 24802 (2021).
27. Y. Li, Y. Qiu, J. Shi, B. Zhang, F. Meng, J. Li, and C. Liu, *ACS Omega* 6, 21465 (2021).
28. X. Wan, and J. Shi, *J. Alloys Compd.* 847, 156472 (2020).
29. X. Wan, M. Chen, Y. Qiu, J. Shi, J. Li, C. Liu, P. Taskinen, and A. Jokilaakso, *Ceram. Int.* 47, 11176 (2021).
30. M. Chen, J. Shi, P. Taskinen, and A. Jokilaakso, *Ceram. Int.* 46, 9183 (2020).
31. Y. Qiu, J. Shi, B. Yu, C. Hou, J. Dong, S. Li, Y. Zhai, J. Li, and C. Liu, *J. Am. Ceram. Soc.* https://doi.org/10.1111/jace.18642 (2022).
32. I.H. Jung, and M.A. Van Ende, *Metall. Mater. Trans. B.* 51, 1851 (2020).
33. B.H. Toby, *J. Appl. Cryst.* 38, 1040 (2005).
34. M.A. Petrova, A.S. Novikova, and V.F. Popova, *J. Mater. Res. Technol.* 12, 2584 (1997).
35. H. Li, R. Xiang, X. Chen, H. Hua, S. Yu, B. Tang, G. Chen, and S. Zhang, *Ceram Int.* 46, 4235 (2020).
36. T. Zienert, and O. Fabrichnaya, *Calphad* 40, 1 (2013).
37. Q. Deng, C. Huang, H. Wang, L. Zhao, and C. Shen, *J. Mater. Sci.* 29, 4035 (2017).
38. W. Lei, W.Z. Lu, D. Liu, and J.H. Zhu, *J. Am. Ceram. Soc.* 92, 105 (2009).
39. T. Yamanaka, *J. Min. Soc. Jpn.* 16, 221 (1983).
40. E.P.T. Barth, *Z. Kristallogr.* 82, 325 (1932).
41. R.L.B. Morosin, *Acta Crystallogr. B* 28, 1040 (1972).
42. R.M.H. Son, B. Kim, Y. Suzuki, and J. Ceram, *Soc. Jpn.* 124, 838 (2016).
43. M. Sobhani, T. Ebadzadeh, and M.R. Rahimipour, *Theor. Appl. Fract Mech.* 85, 159 (2016).
44. A. Shokuhfar, M.N. Samani, N. Naserifar, P. Heidary, and G. Naderi, *Materialwiss. Werkstofftech.* 40, 169 (2009).
45. B.L. Morosin, *Acta Crystal. B* 28, 1040 (1972).
46. Y. Ohya, Y. Kawauchi, and T. Ban, *J. Ceram. Soc. Jpn.* 125, 695 (2017).
47. M. Ilatovskaia, and O. Fabrichnaya, *J. Alloys Compd.* 790, 1137 (2019).
48. D.L. Whitney, *Am. Miner.* 95, 185 (1994).
49. P.G. Eriksson, *Metall. Mater. Trans. B* 24, 795 (1993).